Chemical Physics Letters 549 (2012) 51–57

Contents lists available at SciVerse ScienceDirect

Chemical Physics Letters

journal homepage: www.elsevier.com/locate/cplett

Effects of Au nanoparticles on photoluminescence emission from Si-vacancy in diamond

S. Orlanducci *, I. Cianchetta, E. Tamburri, V. Guglielmotti, M.L. Terranova

Dip. di Scienze e Tecnologie Chimiche, Università degli Studi di Roma Tor Vergata, Via della Ricerca Scientifica, 00133 Roma, Italy

ARTICLE INFO

Article history:
Received 16 April 2012
In final form 14 August 2012
Available online 23 August 2012

ABSTRACT

We studied the coupling of diamond Si color centers with size-controlled Au nanoparticles obtained by chemical routes. The diamond samples, synthesized by Chemical Vapor Deposition, were polycrystalline films or isolated grains. The plasmonic responses of the Au nanoparticles were found to couple with the Ar+ laser frequency or with the frequency of the Si-defects photoluminescence (PL). When the PL of Si optical centers is resonant with the maximum of the Au extinction spectrum, a threshold behavior and a decrease of the PL band FWHM with increasing laser energy is detected, suggesting the transition from spontaneous to stimulated emission.

1. Introduction

The coupling of diamond color centers with plasmonic surfaces and/or structures represents an interesting field of research in solid state physics, material science, and nanophotonics.

It is the stability and the chemical inertness of the all-solid-state sources that distinguishes the diamond color centers from other fluorescent quantum systems affected by photobleaching. More than 500 electronic optical centers have been detected in the absorption and/or luminescence of diamond [1]. Half of them are related to the presence of impurities, in most cases of nitrogen. The negatively charged nitrogen vacancy optical centers (NV^-) have already been largely proposed for quantum-physics application and received a lot of attention in this last decade because of their spin properties [2–4]. Besides that, the optical centers related to Si, Ni, Co or Cr impurities are characterized by remarkable emission properties, such as a very weak vibronic sideband, an extraordinary stability at room temperature, and a high quantum efficiency [5–8]. In particular the Si defects are effortlessly produced in synthetic diamond and can be used as single photon source even in small nanocrystals [9].

While several attempts have been pursued to couple nitrogen vacancy-centers to optical cavities with the aim to enhance spontaneous emission by the Purcell effect [10–13], up to now only few studies have been dedicated to the coupling of optical centers with plasmonic metal nanoparticles. In particular, some papers reported on the plasmonic enhancement of the photoluminescence (PL) due to N-related centers [6,7,14,15], however the published results are often conflicting and overall no further information is added to the current theories [14,15].

The basic idea underlying the present research is the coupling of Si optical centers of different typology of diamond systems with designed plasmonic gold nanoparticles, alternatively coupled with the laser source frequency or with the Si defect photoluminescence frequency.

Our results highlight an interesting threshold behavior of the photoluminescence intensity and a decrease of the band width vs the power source. These experimental features, typical of a laser system, are discussed in term of scattering and of resonant phenomena able to give rise to generate an amplified emission mode.

2. Experimental

Diamond samples were grown using a modified Hot Filament Chemical Vapor Deposition (HFCVD) apparatus equipped with a powder-flowing system specifically designed for a controlled injection of particles [16]. Two kinds of samples were prepared: diamond films (named DF) and isolated diamond grains (named DG) both of them deposited on (100) silicon substrates. Before the diamond deposition, the Si substrates have been scratched with a 0.25 μm diamond paste and ultrasonically cleaned in an acetone bath. The reactant was a methane/hydrogen mixture (1‰$_v$ CH_4 in H_2) activated by a Joule heated Ta filament kept at 2150 ± 10 °C. The total working pressure was 36 ± 1 Torr and the temperature of the substrate holder was fixed at 650 ± 10 °C. Silicon nanoparticles (with a diameter less than 5 nm) were used as additional reactant for the synthesis of DG samples in order to increase the concentration of Si defects [17].

In order to produce tailored gold nanostructures we adopted a chemical synthesis which allowed us to prepare size-controlled nanoparticles in form of colloidal dispersion [18]. The synthesis procedure consists in two operative steps: the preparation of a seed solution followed by a growing phase of the seed. *Preparation*

* Corresponding author.
E-mail address: silvia.orlanducci@uniroma2.it (S. Orlanducci).

0009-2614/$ - see front matter © 2012 Elsevier B.V. All rights reserved.
http://dx.doi.org/10.1016/j.cplett.2012.08.032

of Au seed solution: Twenty milliliters of aqueous solution containing 2.5×10^{-4} M $HAuCl_4$ (Aldrich) and 2.5×10^{-4} M trisodium citrate (Aldrich) was prepared. Next, 0.6 mL of 0.1 M $NaBH_4$ (Aldrich) solution was added to the solution while stirring. The solution turned pink immediately, indicating particles formation. The particles in this solution were used as seeds within 2 h after preparation. *Preparation of growth solution:* Solid cetyltrimethylammonium bromide (CTAB) (Aldrich) was added at 200 mL (0.08 M final concentration) aqueous solution of 2.5×10^{-4} M $HAuCl_4$. The solution was used as a stock growth solution. Next, 2.5 mL of seed solution was added while stirring in the growth solution. By a proper setting of the synthesis time, it was possible to obtain two batches of Au colloidal dispersion characterized by different particles size distribution, centered at 5 nm (NPs) and 300 nm (NPl), respectively.

The spectroscopic features of the as-produced Au nanoparticles were analyzed by standard UV–Vis measurements.

The decoration of the diamond samples with Au nanoparticles was realized by putting Au dispersion drop-wise on the diamond samples surface. Salts and surfactant residues were carefully removed from the surface of the diamond phase by repeated washing treatments. The gold deposition and the following cleaning treatments were repeated many times and PL spectra were collected after each step in order to verify the reproducibility of the system.

The PL spectra were collected at room temperature with a microprobe spectrometer, using a beam focus of 1 μm diameter, a 514.5 nm line of Ar-ion laser as excitation source, and a 600 gr/mm grating spectrometer (iHR550 – HORIBA JOBIN YVON) coupled with a liquid-nitrogen cooled CCD. All the data were acquired using the 514.5 nm laser light, with the aperture slit set at 10 μm to have a PL spectral resolution of 3 cm^{-1}. The laser power was reset during every measurement. For each sample more than 10 spectra were acquired, sampling different points, and then averaged. All PL intensities are reported as a ratio with respect to the fluorescence background. A FESEM Hitachi S4000 apparatus was used for morphological investigation of the Au particles, of the as-produced diamond deposits and of the Au/diamond systems.

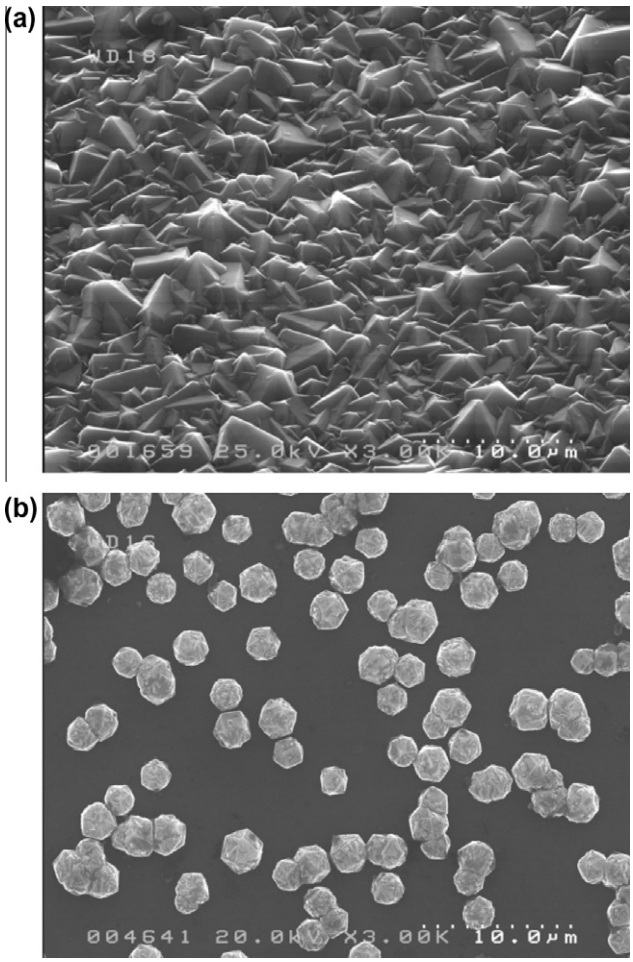

Figure 1. FESEM images: (a) polycrystalline diamond film (DF); (b) isolated diamond grains (DG).

3. Results and discussion

The FESEM images in Figure 1a and b shows the morphology of a diamond film (DF) and of a sample formed of isolated diamond grains (DG), which are representative of all the analyzed samples. A typical polycrystalline topography characterizes all the DF samples (Figure 1a), that have a 15 μm average thickness. The DG samples consist of isolated grains (mean dimensions of some hundred nanometers) having several secondary growths (Figure 1b).

In Figure 2 are shown the typical PL and Raman (insets) spectra of the diamond films (Figure 2a) and of the isolated diamond grains (Figure 2b), taken in the range 540–780 nm. The well shaped peak at 1332 cm^{-1} in the Raman spectra (insets of Figure 2a and b) corresponds to the first order Raman signal of the diamond (Fd3m) phase [19].

In the PL spectra, the broad fluorescence band with a maximum centered at about 580 nm results from the zero phonon line of the NV^0 and the NV^-, together with the strong phonon-coupled bands of the two nitrogen color centers. These centers arise from the nitrogen-vacancy, a very common defect in synthetic diamond grown by CVD [20–22]. The intense signal at 738 nm is the well known photoluminescence peak related to silicon-vacancy complex [23–25]. This PL feature is often shown by CVD diamonds grown on silicon substrates. The methodology of diamond synthesis performed in our labs strongly promotes this occurrence, allowing us to obtain a bright diamond fluorescence in the Near Infrared spectral range [16].

The UV–Vis spectra taken from the colloidal suspensions of the two types of gold nanoparticles, namely NPs (size distribution centered at 5 nm) and NPl (size distribution centered at 300 nm) are shown in Figure 3. The figure displays the absorption spectra of the two colloidal gold suspensions together with the Ar+ laser light line and a typical diamond PL spectrum. It is possible to note a well-shaped band at about 514 nm in the case of the few-nm sized Au particles (sample NPs), whereas a broad band at about 740 nm, superimposed to a broad scattering band, appears in the spectrum of the hundreds-nm sized particles (sample NPl).

The recorded spectra represent the transmission losses due to both absorption and scattering by the Au nanoparticles. It is in fact useful to remind that a metal particle can both dissipate or re-radiate into free space the electromagnetic energy carried by the incident light. These two mechanisms correspond with the well known optical concepts of absorption and scattering, respectively. The relative contribution of these components is determined by the particle size, shape and the intrinsic dielectric response of the metal [26–29]. For small particles, the excitation of plasmonic resonances predominantly leads to absorption of light, whereas scattering becomes the major contribution as the particle diameter approaches the wavelength of visible light.

From inspection of Figure 3 it is clear that the two colloidal suspensions are characterized by two different plasmonic resonances, the first one well-matching with the laser wavelength at 514.5 nm and the second one well-matching with the PL at 738 nm of the Si color centers in diamond. These resonance conditions have been

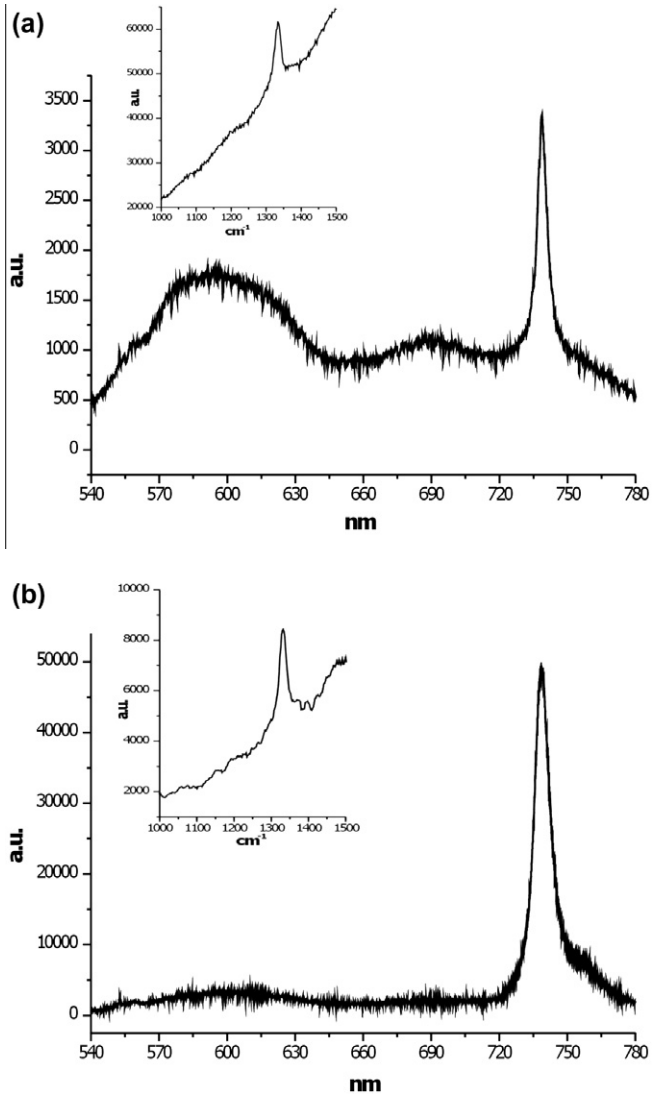

Figure 2. Examples of PL emission spectra in the spectral range 540–780 nm from: (a) diamond film (DF); (b) diamond grains (DG) sample. The insets show Raman spectra (intensity vs the Raman shift) in the spectral range 1000–1500 cm^{-1}.

chosen to perform further spectroscopic experiments in order to study how the Au plasmonic nanoparticles affect the photoluminescence of our diamond structures.

The PL spectra of the bare and Au decorated diamond samples, taken in the spectral range 710–770 nm, are reported in Figure 4. The graphs shown in Figure 4a and b refer to the PL data of the diamond films (DF) and diamond grains (DG), respectively. In each graph the black curve is the PL of the bare diamond, the red curve is the PL of NPs decorated diamond, while the blue curve is the PL of NPl decorated diamond. All the shown PL spectra results from the average of many spectra acquired from different points on the samples surface.

The use of the NPs seems not to enhance the signal for the DF samples (red curve in Figure 4a) but quite to quench it, as seen for the DG samples (red curve Figure 4b). On the other hand, when NPl are used, the PL of the two kinds of diamond samples was found clearly enhanced (blue curves in Figure 4a and b).

The next step was to measure the trend of the PL intensity vs the pumping energy for the NPl decorated DG samples. In Figure 5 is reported the diamond PL vs different laser energies for the bare and for the NPl decorated DG samples. In the inset of Figure 5 is

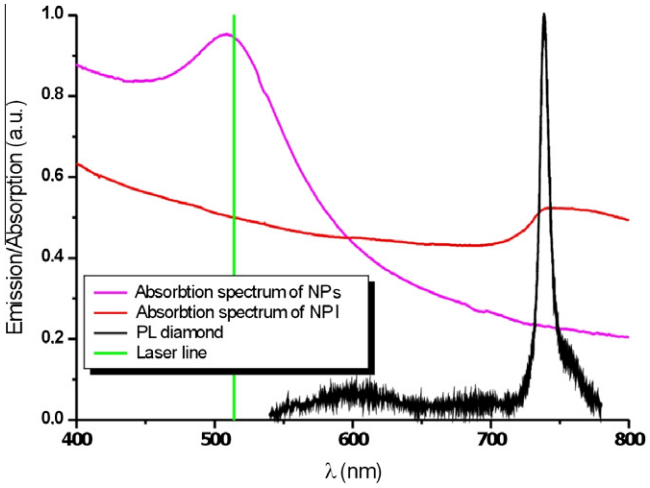

Figure 3. Visible absorption spectra of NPs (magenta line) and NPl (red line) gold nanoparticles. In order to better visualize the matching between photonic and plasmonic components, the laser Ar+ green line and a typical diamond PL spectrum are also reported. (For interpretation of the references to color in this figure legend, the reader is referred to the web version of this Letter.)

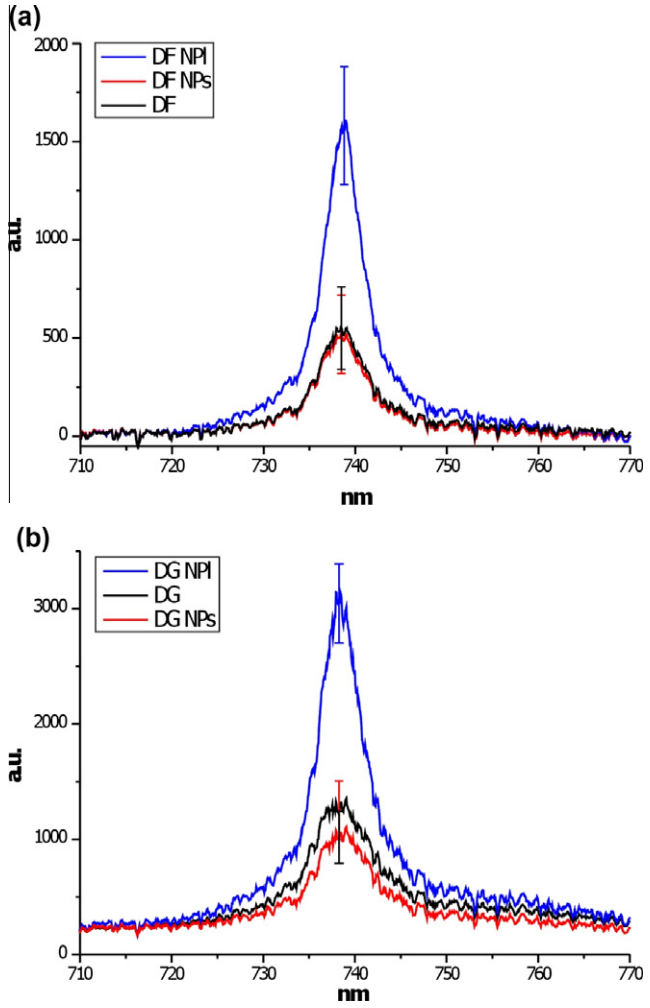

Figure 4. PL averaged spectra in the spectral range 710–770 nm; (a) DF sample (black line), DF sample decorated with NPs (red line) and NPl (blue line); (b) DG sample (black line), DG sample decorated with NPs (red line) and NPl (blue line). For the sake of clarity the error bar is reported only at the maximum. (For interpretation of the references to color in this figure legend, the reader is referred to the web version of this Letter.)

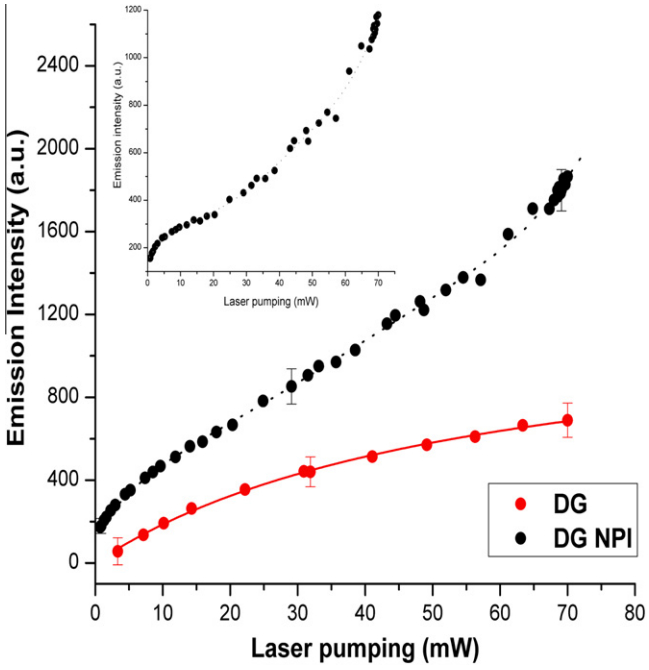

Figure 5. Averaged SiV PL intensities of NPl decorated DG samples (black dots) and bare DG samples (red dots) vs the laser pumping energy. The dependence of the fluorescence on the pump power of a DG sample is well described by the equation $y = Ax/(x + B)$. All the PL intensities are reported as PL/background ratio. The inset shows the SiV PL band for NPl decorated DG samples after the subtraction of the PL of DG bare sample. (For interpretation of the references to color in this figure legend, the reader is referred to the web version of this Letter.)

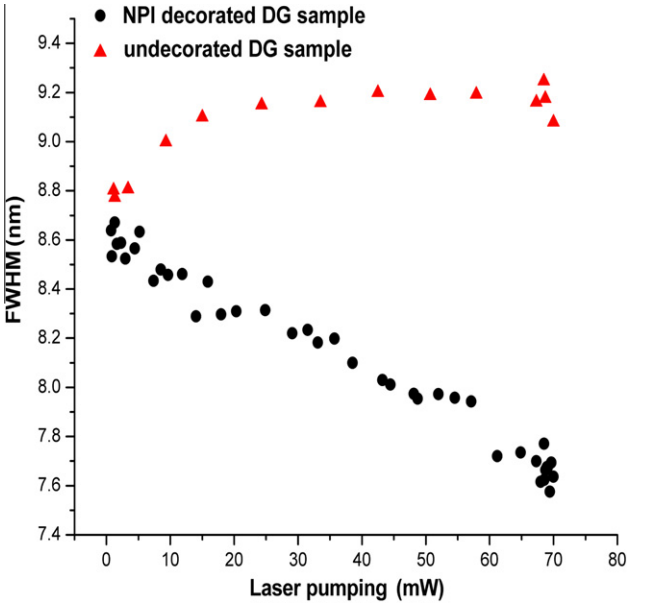

Figure 6. Trend of FWHM of the SiV PL band vs the increasing laser power for NPl decorated DG sample (black dot) and for undecorated DG sample (red triangles). (For interpretation of the references to color in this figure legend, the reader is referred to the web version of this Letter.)

reported the same PL curve for the NPl decorated DG sample after subtraction of the PL from the bare sample.

For the bare diamond sample, the behavior of PL with increasing lasing energy follows the well-known saturation curve (red curve of Figure 5) of a three levels system, related to the laser excited Si defects [30,31]. However, when the diamond sample is decorated with the NPl, the emission behavior (black dots in Figure 5) is clearly modified, displaying an s-like trend. It is clearly seen, in the Figure 5 and in the inset, that beyond a pumping energy threshold of about 15 mW, the PL intensity shows a sharp increase. At the same time, for the NPl decorated sample a clear decreasing of the FWHM of the PL spectra vs the increasing laser power is shown, (Figure 6). In the same Figure 6 it can be seen that this effect does not occur in the PL measurements of bare diamond, that only exhibit a slight increase of the FWHM ascribed to the heating effect induced by the laser beam. The sharp increase of the intensity, together with the decrease of the FWHM (up to the 12%), suggests the occurrence of a transition from spontaneous to stimulated emission as a possible consequence of a lasing mechanism.

In order to better understand the resonant coupling of gold nanoparticles with Si optical center emission as the reason for the detected threshold behavior, we simulated using Mie theory [32,33] the extinction efficiency (Q) (absorption and scattering) of our particles. The curves in Figure 7a were obtained by a simulation based on particles with Log-Normal size distribution centered at 5 nm and 20% Std-Dev, whereas the curves of Figure 7b using particles with Log-Normal size distribution centered at 300 nm and 5% Std-Dev. Such distributions were chosen in agreement with the experimental characteristics of our Au nanoparticles. Both the Figure 7a and b report the extinction (black line), scattering (red line) and absorption (blue line) efficiency (Q) vs the wavelength.

Moreover in order to compare the effect of the medium in our systems, we have simulated the extinction spectra for both the nanoparticles in a medium with refractive index 1 (light source from air), and in addiction for NPl in a medium with refractive index 2.4 (PL from diamond). This last in order to evaluate the scattering and the absorption of the emitted light (738 nm PL) that came from the bulk diamond and interact with the NPl at the interface air–diamond.

The theoretical extinction spectrum of NPs (Figure 7a), almost completely superimposed to the Q_{abs} line, exhibits a maximum centered at 510 nm, that is very close to the absorption maximum in the UV–Vis spectrum of NPs. As expected, the scattering contribution is very low and therefore the major contribution to the extinction coefficient is given by the absorption. Overall it should be stressed that the 5 nm sized particles are characterized by very low efficiency values.

Conversely, for the 300 nm sized particles (Figure 7b) the major contribution to the extinction coefficient, especially in the range 500–1000 nm, is given by the scattering, and exhibits a maximum at about 740 nm. Note that in this case the scattering efficiency is very high and that the Q_{sca}/Q_{abs} ratio is about 15 at 740 nm.

In Table 1 are reported, for NPs and NPl, the calculated extinction and scattering efficiency, Q, at 514 and 738 nm together with the scattering strength parameter $|k|ls$, where k is the wavevector of the light, and the scattering mean free path (ls).

This last quantity is given by: $ls = 1/\rho\pi r^2 Q_{sca}$, where ρ is the volume density of particles on diamond surface, estimated to be about $10000/\mu m^3$ in the case of NPs and $2/\mu m^3$ for the larger particles NPl; and r is the particle radius. Also in this case we used air as the medium for both the 514 and 738 nm wavelengths, and diamond for the 738 nm wavelength.

The present results suggest some interesting speculations.

First of all our systems appear to be similar to a plasmonic enhanced random laser. In a random laser the multiple scattering phenomenon provides the feedback mechanism that keeps the light circulating in the gain medium long enough so that the gain exceeds the losses. In these systems, metal nanoparticles may enhance the lasing efficiency by intensifying the scattering strength

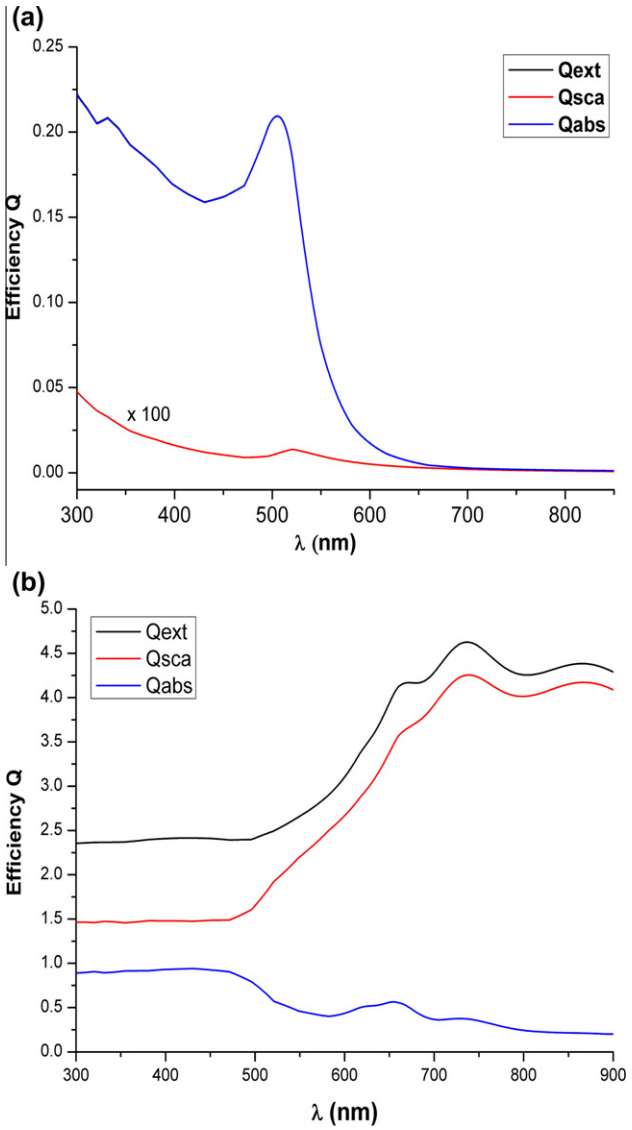

Figure 7. Efficiency (Q) of simulated extinction (black line), scattering (red line) and absorption (blue line) vs the wavelength; (a) particles with Log-Normal size distribution centered at 5 nm and 20% Std-Dev; (b) particles with Log-Normal size distribution centered at 300 nm and 5% Std-Dev. (For interpretation of the references to color in this figure legend, the reader is referred to the web version of this Letter.)

and/or the dye fluorescence by means of an enhanced localized field. Incoherent and coherent feedback have been demonstrated and related both to scattering and plasmon efficiency [34–37].

As it has been evidenced by the simulated extinction spectrum reported in Figure 7b and the value in the Table 1, NPl are very efficient in scattering the 738 nm radiation (the Si PL emission). However it is necessary to emphasize that the system operates in a weak scattering regime ($kl > 1$), due to the low volumetric density of Au nanoparticles. Despite that, the PL of the Si-optical centers in presence of NPl definitively shows a threshold behavior in regard to the increase of the PL intensity and the linewidth narrowing.

Another interesting observation can be done about the remarkable scattering contribution given by these particles in the wavelength region ranging from 500 to 1000 nm. This effect could be responsible of the amplification of the fluorescence signals and of the background.

Anyway it would be simplistic to explain the trend shown by the PL vs pumping energy only as due to a scattering-induced enhancement of the laser source intensity, or to a surface plasmon (SP) field enhancement.

In fact even if both these phenomena could explain the PL amplification detected at low laser pumping energy, a feedback mechanism has to be invoked to explain the threshold behavior.

Several authors have demonstrated that metal-nanoparticles dye random laser systems not only operate better than the dielectric based random lasers, but that they also work at extremely weak scattering strengths, as a result of the highly localized optical modes due to surface plasmon resonance (SPR) [37]. Moreover the lasing properties were dramatically improved when the SPR or the 'scattering resonance' wavelength of the metal particles overlapped the dye emission [35]. Anyway even if SP seems to play an impressive role, it has not been clarified yet which feedback mechanism is implied in the very weak scattering regime.

It would be useful to describe our system as a result of the scattering of the PL emission of the Si center from a gold particle at the diamond/air interface. In Figure 8a the angular dependence of the NPl scattering intensities of the 738 nm wavelength in $n = 1$ (blue curve) and $n = 2.4$ (red curve) medias, are reported. This very simplified approach to the scattering from particles at the interface is justified by the particles size and well described the backscattering phenomenon. As highlighted by the polar graph, the 738 nm wavelength is very efficiently backscattered by NPl, allowing a resonant energy transfer between the plasmonic structure and the excited level of the diamond SiV.

In our NPl/diamond systems we find that the plasmon resonance and the scattering resonance of the particles are perfectly coupled with the Si centers PL emission, as occurs for the metal particles and the dye emission of the plasmonic enhanced random lasers.

The resonance between the energy levels of the Si color centers and the plasmonic levels related to the larger gold nanoparticles can further explain the narrowing of the bandwidth. The resonant energy transfer between the excited level of the SiV and the plasmonic structure would allow a repopulation of the excited state and a subsequent lengthening of the life time. As is it well known, the longer the life of a state, the more monochromatic the emission line. The repopulation of the Si defect level provided by the scattering properties of the gold nanoparticles would then supply a longer lifetime and a strong narrowing of the photoluminescence emission line.

A scheme of such mechanism is sketched in Figure 8b. In Figure 8c and d is reported also a graphical summary of the PL results obtained decorating isolated diamond grains with NPs and NPl Au particles, respectively.

Table 1
Calculated extinction and scattering efficiency at 514 and 738 nm together with scattering mean free path (ls) and scattering strength parameter $|k|ls$ for NPs and NPl particles.

	Wavelength (nm)	Extinction efficiency Q_{ext}	Scattering efficiency Q_{sca}	Scattering mean free path ls (μm)	Scattering strength $|k|ls$
NPs (air)	514	0.20	1×10^{-4}	13000	10^5
NPs (air)	738	0.15	4×10^{-3}	400	10^4
NPl (air)	514	3.8	2.4	3	36
NPl (air)	738	3.3	2.2	3	27
NPl (diamond)	738	4.8	4.4	1	10

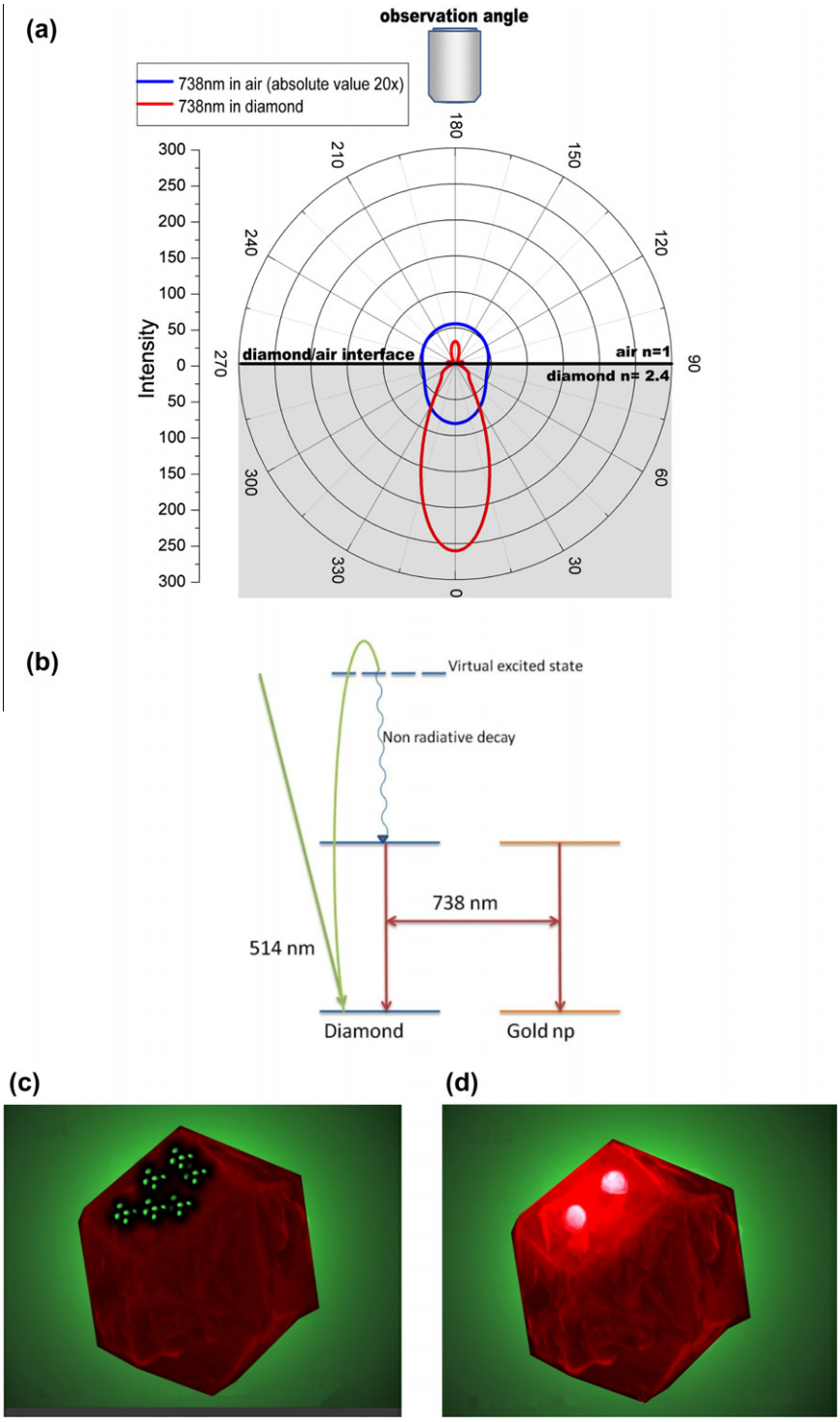

Figure 8. (a) Polar graph of the scattering intensities for NPl calculated for the 738 nm wavelength and using as medium air (curve blue) and diamond (curve red). (b) Proposed feedback mechanism; (c and d) graphical summary of the PL results obtained decorating isolated diamond grain with NPs and NPl Au particles. The (b and c) images illustrate the quenching and the lasting effects, respectively. (For interpretation of the references to color in this figure legend, the reader is referred to the web version of this Letter.)

4. Conclusions

The present research concerns the coupling of Si optical centers of various diamond systems with properly designed plasmonic Au nanoparticles. A high concentration of Si defects in the diamond lattice is achieved by inserting Si nanoparticles during the CVD growth of diamond, and batches of size-controlled Au nanoparticles are produced using chemical routes. In our experiments the excitation of the diamond PL Si defects (emission at 738 nm) is provided by a laser line at 514.5 nm, whereas the prepared Au nanoparticles (NPs and NPl) have a maximum in the extinction spectrum at about 514 and 740 nm, thus resulting perfectly coupled with the laser source wavelength and with the 738 nm PL band, respectively.

When diamonds are coupled with the larger gold nanoparticles, the PL of diamond Si optical center shows an interesting laser-like behavior, with a threshold at about 15 mW, and a decrease of the FWHM of PL with increasing laser energy. The two results together suggest the transition from spontaneous to stimulated emission as a consequence of a lasing mechanism.

Theoretical calculations highlighted a weak scattering regime and, similarly with plasmonic enhanced random laser systems working in a weak scattering regime, also in this case SP seems to play an impressive role. Feedback mechanism in our laser-like systems could be rationalized considering the resonant energy transfer between the excited level of the Si defect and the plasmonic structure, with a consequent repopulation of the excited state and a consequent lengthening of the lifetime. The repopulation of the Si defect levels provided by the gold nanoparticles may explain the transition from amplified to stimulated emission as a result of the highly efficient backscattering phenomenon.

Time resolved spectroscopy experiments would be anyway useful to better understand the phenomena involved in our systems. Moreover an optimization of the plasmonic and scattering response could be achieved by a proper choice of both shape and size distribution of the Au particles.

Nevertheless the present Letter can be considered a proof of principle for innovative solid state laser and the relevant performance highlighted for these diamond/Au systems opens an exciting prospective for the development of novel diamond based nanophotonic devices.

References

[1] A.M. Zaitsev, Phys. Rev. B 61 (2000) 12909.
[2] P. Neumann et al., Science 320 (2008) 1326.
[3] I. Vlasov et al., Small 6 (2010) 687.
[4] Ch. Kurtsiefer, S. Mayer, P. Zarda, H. Weinfurter, Phys. Rev. Lett. 85 (2000) 290.
[5] A.M. Edmonds, M.E. Newton, P.M. Martineau, D.J. Twitchen, S.D. Williams, Phys. Rev. B 77 (2008) 245205.
[6] K. Iakoubovskii, A. Stesmans, Phys. Rev. B 66 (2002) 195207.
[7] I. Aharonovich, S. Prawer, Diamond Relat. Mater. 19 (2010) 729.
[8] K. Iakoubovskii, G. Davies, Phys. Rev. B 70 (2004) 245206.
[9] I.I. Vlasov et al., Adv. Mater. 21 (2009) 808.
[10] J. Wolters et al., Appl. Phys. Lett. 97 (2010) 141108.
[11] B. Patton, J.L. O'Brien, Nat. Photonics 5 (2011) 256.
[12] I. Bulu, T. Babinec, B. Hausmann, J.T. Choy, M. Loncar, Opt. Express 19 (2011) 5268.
[13] J.T. Choy et al., Nat. Photonics 5 (2011) 738.
[14] M. Barth, S. Schietinger, T. Schroder, T. Aichele, O. Benson, J. Lumin. 130 (2010) 1628.
[15] T.S. Lim et al., Phys. Chem. Chem. Phys. 11 (2009) 1508.
[16] S. Orlanducci, V. Sessa, E. Tamburri, M.L. Terranova, M. Rossi, S. Botti, Surf. Coat. Technol. 201 (2007) 9389.
[17] M.L. Terranova, D. Manno, M. Rossi, A. Serra, E. Filippo, S. Orlanducci, E. Tamburri, Crys. Growth Des. 9 (2009) 1245.
[18] C.J. Murphy et al., J. Phys. Chem. B 109 (2005) 13857.
[19] S. Prawer, R.J. Nemanich, Philos. Trans. R. Soc. Lond. A 362 (2004) 2537.
[20] V.S. Vavilov, A.A. Gippius, A.M. Zaitsev, B.V. Deryagin, B.V. Spitsyn, A.E. Aleksenko, Sov. Phys. Semicond. 14 (1980) 1078.
[21] T. Collins, M. Stanley, G.S. Woods, J. Phys. D 20 (1987) 969.
[22] L.H. Robins, L.P. Cook, E.N. Farabaugh, A. Feldman, Phys. Rev. B 39 (1989) 13367.
[23] C.D. Clark, H. Kanda, I. Kiflawi, G. Sittas, Phys. Rev. B 51 (1995) 16681.
[24] H. Sternschulte, K. Thonke, R. Sauer, P.C. Munzinger, P. Michler, Phys. Rev. B. 50 (1994) 14554.
[25] Y. Zhu, H. Wang, P.P. Ong, J. Phys. D: Appl. Phys. 33 (2000) 2687.
[26] B.J. Messinger, K.U. von Raben, R.K. Chang, P.W. Barber, Phys. Rev. B 24 (1981) 649.
[27] J.R. Lakowicz, Anal. Biochem. 337 (2005) 171.
[28] P.K. Jain, K.S. Lee, I.H. El-Sayed, M.A. El-Sayed, J. Phys. Chem. B 110 (2006) 7238.
[29] K. Kelly, E. Coronado, L.L. Zhao, G.C. Schatz, J. Phys. Chem. B 107 (2003) 668.
[30] C. Wang, C. Kurtsiefer, H. Weinfurter, B. Burchard, J. Phys. B: At. Mol. Opt. Phys. 39 (2006) 37.
[31] E. Neu, D. Steinmetz, J. Riedrich-Möller, S. Gsell, M. Fischer, M. Schreck, C. Becher, New J. Phys. 13 (2011) 025012.
[32] G. Mie, Ann. Phys. 25 (1908) 377.
[33] C.F. Bohren, D.R. Huffman, Absorption and Scattering of Light by Small Particles, Wiley Interscience, New York, 1983.
[34] G.D. Dice, S. Mujumdar, A.Y. Elezzabi, Appl. Phys. Lett. 86 (2005) 131105.
[35] O. Popov, A. Zilbershtein, D. Davidov, Appl. Phys. Lett. 89 (2006) 191116.
[36] J.U. Kang, Appl. Phys. Lett. 89 (2006) 221112.
[37] X. Meng, K. Fujita, Y. Zong, S. Murai, K. Tanaka, Appl. Phys. Lett. 92 (2008) 201112.